Identification of quantitative trait loci (QTLs) regulating leaf SPAD value and trichome density in mungbean (*Vigna radiata* L.) using genotyping-by-sequencing (GBS) approach

Nikki Kumari[1,*], Gyan Prakash Mishra[1], Harsh Kumar Dikshit[1], Soma Gupta[1], Anirban Roy[2], Subodh Kumar Sinha[3], Dwijesh C. Mishra[4], Shouvik Das[1], Ranjeet R. Kumar[5], Ramakrishnan Madhavan Nair[6] and Muraleedhar Aski[1,*]

[1] Genetics, Indian Agricultural Research Institute, New Delhi, Delhi, India
[2] Plant Pathology, Indian Agricultural Research Institute, New Delhi, Delhi, India
[3] Biotechnology, National Institute of Plant Biotechnology, New Delhi, Delhi, India
[4] Agricultural Bioinformatics, Indian Agricultural Statistics Research Institute, New Delhi, Delhi, India
[5] Division of Biochemistry, Indian Agricultural Research Institute, New Delhi, Delhi, India
[6] ICRISAT, World Vegetable Center, South Asia, ICRISAT Campus, Patancheru, Hyderabad, India
[*] These authors contributed equally to this work.

ABSTRACT

Quantitative trait loci (QTL) mapping is used for the precise localization of genomic regions regulating various traits in plants. Two major QTLs regulating Soil Plant Analysis Development (SPAD) value (*qSPAD-7-1*) and trichome density (*qTric-7-2*) in mungbean were identified using recombinant inbred line (RIL) populations (PMR-1×Pusa Baisakhi) on chromosome 7. Functional analysis of QTL region identified 35 candidate genes for SPAD value (16 No) and trichome (19 No) traits. The candidate genes regulating trichome density on the dorsal leaf surface of the mungbean include *VRADI07G24840, VRADI07G17780*, and *VRADI07G15650,* which encodes for ZFP6, TFs bHLH DNA-binding superfamily protein, and MYB102, respectively. Also, candidate genes having vital roles in chlorophyll biosynthesis are *VRADIO7G29860, VRADIO7G29450*, and *VRADIO7G28520*, which encodes for s-adenosyl-L-methionine, FTSHI1 protein, and CRS2-associated factor, respectively. The findings unfolded the opportunity for the development of customized genotypes having high SPAD value and high trichome density having a possible role in yield and mungbean yellow vein mosaic India virus (MYMIV) resistance in mungbean.

Subjects Agricultural Science, Bioinformatics, Genomics, Molecular Biology, Plant Science
Keywords Candidate genes, Chlorophyll content, Green gram, Marker assisted selection, Trichomes

Submitted 29 August 2023
Accepted 4 December 2023
Published 21 February 2024

Corresponding authors
Gyan Prakash Mishra, gyan.gene@gmail.com
Harsh Kumar Dikshit, harshgenetic-siari@gmail.com

Academic editor
Ravinder Kumar

Additional Information and Declarations can be found on page 16

DOI **10.7717/peerj.16722**

How to cite this article Kumari N, Mishra GP, Dikshit HK, Gupta S, Roy A, Sinha SK, Mishra DC, Das S, Kumar RR, Nair RM, Aski M. 2024. Identification of quantitative trait loci (QTLs) regulating leaf SPAD value and trichome density in mungbean (*Vigna radiata* L.) using genotyping-by-sequencing (GBS) approach. *PeerJ* **12**:e16722 http://doi.org/10.7717/peerj.16722

INTRODUCTION

Mungbean (*Vigna radiata* L.) is a leguminous crop, cultivated widely in various regions including Africa, South America, Australia, and Asian countries. It contains a diverse range of protein, fiber, antioxidants, and phytonutrients (*Reddy et al., 2021*). It is consumed in different forms like whole seeds, flour, sprouts, microgreens, *etc.*, making it an important source of dietary protein (*Priti et al., 2021*; *Priti et al., 2022*). The average World productivity of mungbean ranges between 2.5 and 3.0 t/ha, whereas mean Indian yield is only 0.5 t/ha (*All India Coordinated Research Project (AICRP), 2022*). This can be attributed to various factors, including biotic and abiotic constraints. Extensive research has been conducted on traits governing responses to various stresses, yet certain traits like soil plant analysis development (SPAD) value and trichome density have received limited attention in mungbean. On contrary, these have been extensively studied in soybean and other crops providing valuable insights into their genetic control and functional significance (*Yu et al., 2020*; *Angira et al., 2022*).

The leaf chlorophyll content is instrumental in light absorption and subsequent conversion of solar energy into chemical energy through photosynthesis (*Singhal et al., 2012*). It plays a crucial role in determining photosynthetic efficiency and yield (*Sakowska et al., 2018*). Traditionally, the assessment of leaf chlorophyll content involved extract-based quantification through spectrophotometric measurements of chlorophyll a and chlorophyll b (*Carter & Knapp, 2001*; *Dhanapal et al., 2016*). In contrast, SPAD method is a non-invasive, rapid, and cost-effective way of estimating the relative chlorophyll content using a portable SPAD chlorophyll meter (*Lombard et al., 2010*). A high SPAD value indicates a lower degree of photoinhibition during photosynthesis (*Yu et al., 2022*) and vice versa. A positive correlation between leaf chlorophyll content and seed yield was demonstrated in soybean, especially during reproductive stage (*Ma, Morrison & Voldeng, 1995*). However, such studies are lacking in mungbean.

Trichomes are specialized structures on the dorsal leaf surface that have significant intraspecific variability (*Chen et al., 2021*). Trichome density affects the insect feeding behavior, oviposition patterns, and nourishment of larvae (*Schillinger Jr & Gallun, 1968*; *Roberts et al., 1979*). Trichomes house specialized glands emitting terpenes, phenolics, alkaloids, and other olfactory and or gustatory deterrents which minimizes thrips and whiteflies infestation and thereby has a role in YMD resistance (*Kivimaki et al., 2007*; *Chen et al., 2021*; *Yasmin et al., 2022*).

Trichomes also acts as a physical barrier against biotic and abiotic stresses (*Kariyat et al., 2018*). In *Arabidopsis thaliana*, nearly 40 genes have been identified governing trichome density (*Mauricio, 2005*; *Atwell et al., 2010*). The key regulators include R2R3 MYB transcription factor GLABRA 1 (GL1), the basic helix-loop-helix (bHLH) transcription factor GLABRA 3/ENHANCER OF GLABRA 3 (GL3/EGL3), and the pleiotropic WD40 repeat protein TRANSPARENT TESTA GLABRA 1 (TTG1), collectively forming the MYB-bHLH-WDR (MBW) complex, a central component of the trichome initiation pathway (*Kirik et al., 2004*; *Zhao et al., 2008*). Significant progress has been made in understanding the genetic basis of trichome initiation and development in *Arabidopsis*, and soybean (*Li et*

al., 2021), however, research in mungbean remains very limited. Advancements in genetic mapping helped in the identification of robust single nucleotide polymorphism (SNP) markers (*Grant et al., 2011*) which helped in the construction of high-density genetic maps (*Qi et al., 2014*; *Jiang et al., 2020*).

This study aims to map the QTLs regulating SPAD value and trichome density in an RIL population derived from the cross between Pusa Baisakhi and PMR-1, which exhibit distinct responses for these traits. Pusa Baisakhi is characterized by low trichome density and light-colored leaves, while PMR-1 displays higher trichome density on the dorsal leaf surface and possesses darker leaves. The aim of this study was to map the QTLs regulating SPAD value and trichome density in mungbean using recombinant inbred line (RIL) population using GBS based genetic map (*Mathivathana et al., 2019*; *Chen et al., 2022*).

MATERIAL AND METHODS

Plant materials, mapping population, and trait measurement

The RIL population, consisting of 166 lines, was developed at the Indian Agricultural Research Institute (IARI) in New Delhi, India by crossing Pusa Baisakhi and PMR-1. Pusa Baisakhi is known for its low SPAD value (an indirect measurement of chlorophyll content) and low trichome density. On the other hand, PMR-1 exhibits a high SPAD value and high trichome density. To create the RIL population, the F_1 plants were self-pollinated to produce F_2 population and from F_2, 166 $F_{7:8}$ lines were developed using the single seed descent (SSD) method. This process involves selecting individual plants from each generation and allowing them to self-pollinate, followed by selecting a single pod from each plant for the next generation. Each RIL genotype was planted in a 4-meter row and spacing between each row and individual plants was maintained at 30 cm and 10 cm, respectively, allowing for approximately 40 plants in each row. From every row, five plants were randomly selected for the measurement of SPAD values and trichome density. The parents and RILs were screened for their SPAD values and trichome density during 2020 (July–November) and 2021 (July–November) in a randomized complete block design with two replications at the Indian Agricultural Research Institute (IARI), New Delhi, India (28.7041°N, 77.1025°E; 228.61 m above mean sea level). Field management followed the standard recommended mungbean cultivation practices for the area.

SPAD value determination

The SPAD meter measures non-destructively the light transmittance of the leaf at 650 and 940 nm in the red and infrared wavelengths, providing a numerical output representing leaf greenness and chlorophyll concentration (*Markwell, Osterman & Mitchell, 1995*). The SPAD value was used as an indicator of the relative chlorophyll content in mungbean leaves. Five healthy plants situated in the middle of each row were randomly selected for SPAD value measurement using SPAD-502 Chlorophyll Meter at 45 DAS during 08:00 am to 11:00 am (*Wang et al., 2020*). The SPAD was measured at the top, middle, and bottom of a leaflet of the third leaf from the top in three replications (*Guang-Jun et al., 2010*). The mean SPAD value was designated as TSP (top site portion), MSP (middle site portion),

and BSP (bottom site portion), respectively. Additionally, the average SPAD values (ASP) were determined by calculating the mean of TSP, MSP, and BSP.

Trichome density characterization

The trichome density was studied using five randomly selected plants per row by taking one fully expanded leaf (mid portion) at (i) seedling stage and (ii) after anthesis (*Chen et al., 2021*). The data was recorded using a compound microscope equipped with an ocular scale and bright field optics (10×). Before mounting on a glass slide, the upper epidermis (middle portion) of leaf was carefully coated with a thin layer of nail varnish and after five minutes, the film was peeled from the surface using a piece of transparent sticky tape. The scale of '0' (any short and sparse trichome) to '3' (long and dense trichome) was used for the measurement of trichome density.

Statistical analysis

R software (*R Core Team, 2013*) was employed for comprehensive analysis. This encompassed ANOVA, Pearson phenotypic correlation computation, density plot assessment, and scatter plot visualization, Providing valuable insights into the data's variance, associations, distribution, and inter-variable relationships.

DNA extraction and genotyping by sequencing

The genomic DNA isolated using cetyltrimethyl ammonium bromide (CTAB) method (*Lodhi et al., 1994*) from the young leaves of parental lines and 166 RIL population were used for the preparation of GBS libraries (*Elshire et al., 2011*). In brief, 100 ng DNA was digested for 4.0 h at 75 °C with ApeKI (New England Biolabs, Ipswitch, MA) in 20 μL volume containing 1 × NEB Buffer3 and 3.6U ApeKI. The purified 168-plex final DNA library was quantified using Bioanalyzer (Agilent Technologies) and was sequenced on Novaseq 6000 (Illumina® Inc., San Diego, CA, USA). Library construction and sequencing were done by NGB Diagnostics Pvt Ltd (India) and SNPs were identified. Variant calling was done using UGBS-GATK pipeline (version v3.6, https://gatk.broadinstitute.org/hc/en-us). Further SNPs were filtered based on minor allele frequency (MAF) of 5%, being present in at least 50% of the population, the proportion of heterozygosity, and polymorphism information,

Genetic map construction and QTL analysis

The genetic linkage map of the RIL population was constructed based on the SNP markers identified through GBS and was used to map the QTLs for the SPAD value and trichome density traits. The high-quality SNPs were evaluated against the expected Mendelian segregation ratio using chi-square analysis for the genetic linkage map construction. The SNPs displaying distorted segregation ratios were excluded from the analysis and high-quality SNPs were used to construct the genetic map using JoinMap version 4.1 (*Stam, 1993*). A rippling algorithm having a window size of 1 was applied which improved the marker order by iteratively adjusting the marker positions within the linkage groups. To facilitate the comparative analysis, the marker distances were converted into centiMorgans (cM) using Kosambi's mapping function. Linkage groups (LGs) were visually represented

using Mapchart v2.32 (*Voorrips, 2022*). The order of SNPs on the genetic map was compared with their physical position on the mungbean reference genome downloaded from Ensembl Plants (release 54).

The QTL analysis was performed using composite interval mapping functions embedded in QTL IcIMapping v4.2 software (*Zeng, 1993*). To establish the statistical significance of the identified QTLs, a LOD threshold was calculated by performing 1000 permutations at $P \leq 0.05$ and phenotypic variance explained (PVE) value $\geq$10%. The nomenclature for QTL was like *qSPAD-7-1* where "qSPAD" represents the QTL for the SPAD value and 7-1 represents the first QTL on chromosome 7. For SPAD value, 142 RILs; while for trichome density, 166 RILs were used for the QTL analysis.

Candidate gene and digital expression analysis

The genetic linkage map of the RIL (Pusa Baisakhi × PMR-1) was integrated with the physical map of the mungbean reference genome for the determination of physical locations of markers flanking the QTLs of interest. The mapping intervals of the detected QTLs were identified, and gene models falling within these intervals were retrieved from Ensembl Plants (https://plants.ensembl.org/biomart/martview), and the NCBI genome data viewer (GCF_000741045.1). In addition, other methods used include ShinyGO 0.77 analysis, DAVID, and gene annotation data. Genes known to be involved in SPAD value and trichome development, as reported in *Arabidopsis*, were collected from the *Arabidopsis* Information Resource (TAIR) (https://www.arabidopsis.org/index.jsp). The *Arabidopsis* genes were then used as queries in BLASTN search against the mungbean genome assembly to identify the candidate genes. Based on the well-characterized functions of these orthologous genes, candidate genes regulating SPAD value and trichome density were identified. Digital gene expression analysis was done using *Arabidopsis* orthologs and an Expression Angler was used to investigate their localized expression patterns (*Austin et al., 2016*; *Reddy et al., 2020*).

RESULTS

Evaluation of phenotypic variation

The parental genotypes and RILs displayed substantial variations in SPAD value and trichome density across two years (Table 1; Fig. S1) suggesting the presence of considerable diversity for these traits. Table 1 summarizes key descriptive statistics for SPAD value (chlorophyll content) and trichome density in parents (Pusa Baisakhi and PMR-1) and RIL populations. Some RILs showed lower or higher values than the parents for SPAD value and trichome density, indicating transgressive segregation during both the studied years. The difference between parents' SPAD values is 47.29, while trichome density ranges from 0 to 3. An analysis of the Pearson correlation coefficient indicated a non-significant positive correlation between SPAD value and trichome density ($r^2 = 0.119$) in the $F_{7:8}$ RILs (Fig. 1).

QTL identification for SPAD value and trichome

In total, 107.662 Gb raw data were generated and after cleaning 100.748 Gb high-quality data was utilized for downstream analysis. After adapter trimming, 98.33 Gb data was

Table 1 Descriptive statistics for SPAD value (chlorophyll content) and trichomes in parents and RIL popuilation.

Trait	Parents		Difference (parents)	RIL Population			
				$F_{5:6}$ lines		$F_{7:8}$ lines	
	Pusa Baisakhi	PMR-1		Range	Mean ± SD	Range	Mean ± SD
SPAD value	2.39	49.68	47.29	1.75-43.66	24.01 ± 8.80	2.52-59.43	25.05 ± 9.9
Trichome	0	3	3	1-3	2.0 ± 0.59	1-3	2.11 ± 0.67

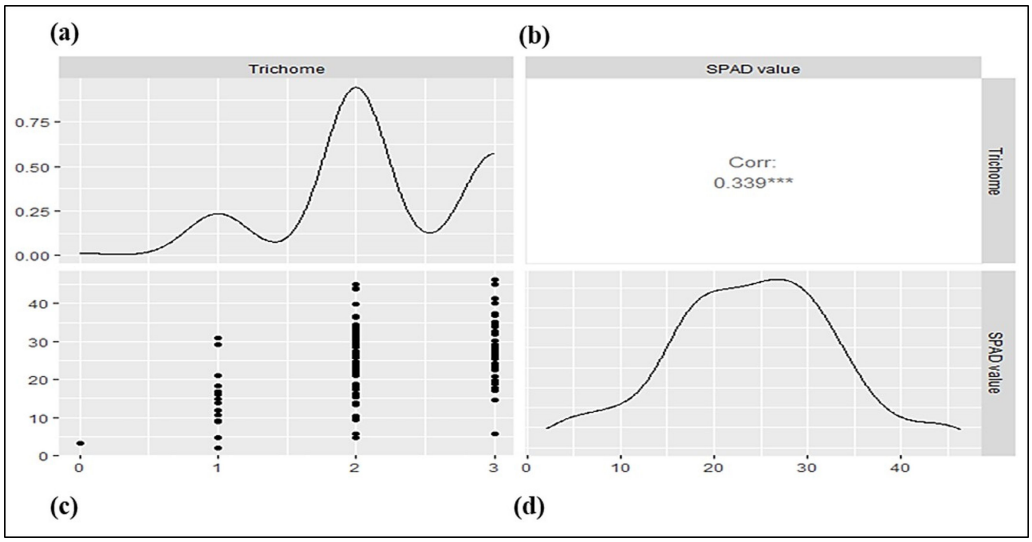

Figure 1 **The correlation between trichome density and SPAD values in a mungbean RIL population.** (A) Density plot for SPAD value. (B) Pearson's phenotypic correlation between SPAD and trichome density. (C) Scatter plot. (D) Density plot for trichome density.

Full-size DOI: 10.7717/peerj.16722/fig-1

obtained from both parents and 166 RILs population which was used for final analysis. Initial screening yielded 6797 SNPs, and after applying various stringent selection criteria, the SNPs were reduced to 1,730 numbers. The genetic map was comprised of 1,730 SNPs, distributed across 11 linkage groups (LGs) ranging from 42.482 cM to 74.321 cM, and the marker density varied from 105 to 345. Overall, the genetic map covered a total genetic distance of 596.1 cM, with an average marker interval of 0.345 cM.

QTL analysis was conducted for SPAD value and trichomes using a linkage map having 1730 SNPs covering 11 chromosomes using inclusive composite interval mapping (ICIM) (Fig. 2). The results of the QTL analysis revealed one QTL for SPAD value and three QTLs for trichome density over two years (Table 2). The LOD scores of these QTLs ranged from 2.67 to 6.29 (Fig. 3), while the phenotypic variance explained ranged from 6.38 to 14.0%, indicating the proportion of phenotypic variation accounted for by the respective QTLs.

In the year 2020, ICIM analysis identified three QTLs related to SPAD value and trichome traits in an RIL population. A major QTL named, *qSPAD-7-1* (marker intervals VR7:55078511 and VR7:49782591) was found regulating the SPAD value on chromosome 7, which explained 11.55% of PVE. Two minor QTLs governing trichome density were

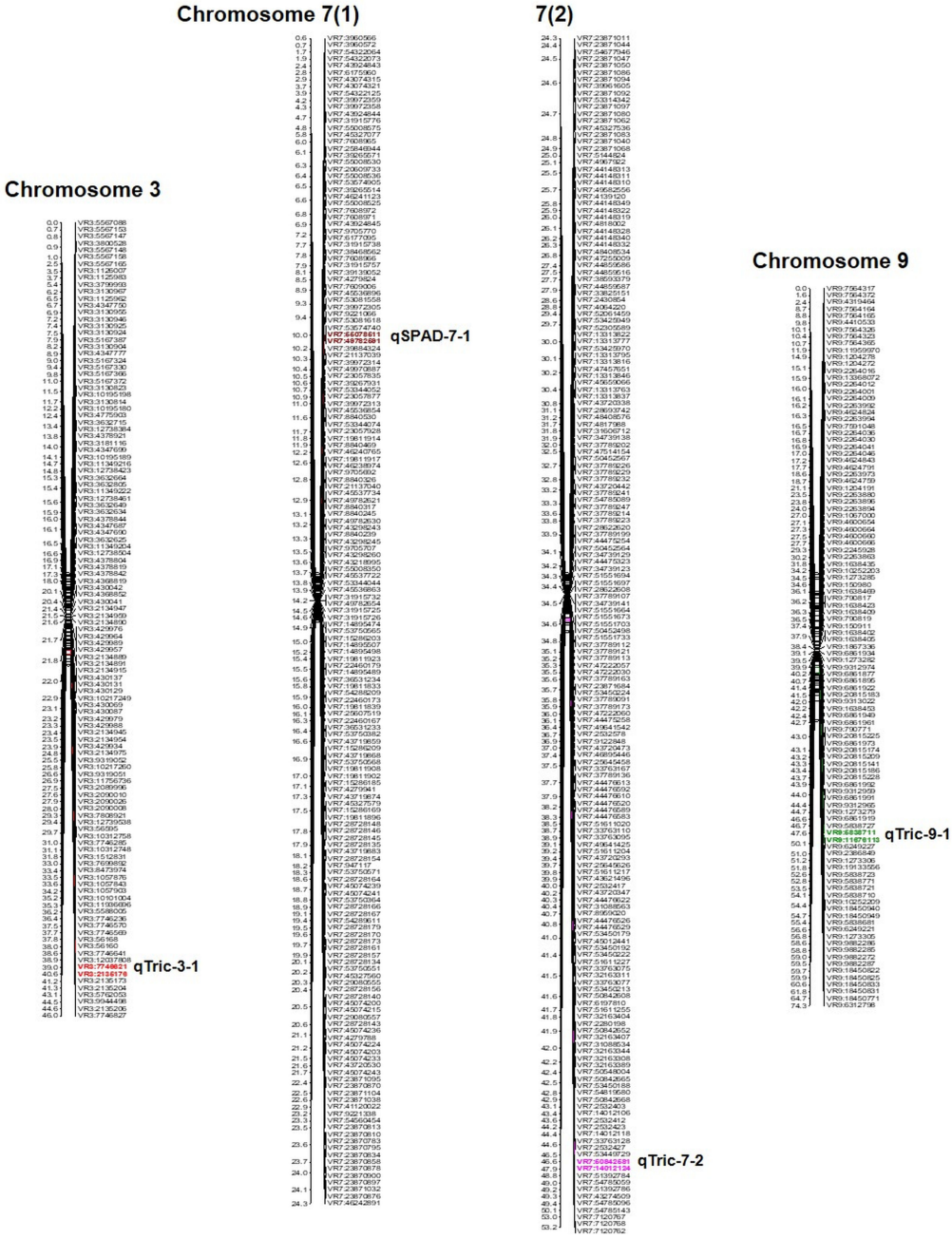

Figure 2 **Position of QTLs regulating trichome and chlorophyll content on chromosomes 03, 07, and 09 in a mungbean RIL mapping population.**

Full-size DOI: 10.7717/peerj.16722/fig-2

identified on chromosome 3 (*qTric-3-1*; 6.38% PVE; marker interval VR3:7746621–VR3:2135176) and chromosome 9 (*qTric-9-1*; 6.74% PVE; marker intervals VR9:5838711 and VR9:11676113) (Fig. 2). The identified QTLs were found contributed by the parent PMR-1 for both SPAD value (*qSPAD-7-1*) and trichome density (*qTric-3-1*, *qTric-9-1*).

Table 2 Details of QTLs governing SPAD value and trichomes in a mungbean RIL population.

Traits	QTL name	Year	LG[a]	Position[b] (cM)	Interval[c] (bp)	LOD[d]	PVE[e] (%)	A[f]
SPAD value	*qSPAD-7-1*	2020	7	10	VR7:55078511-VR7:49782591	3.49	11.55	3.35
	qSPAD-7-1	2021	7	10	VR7:55078511-VR7:49782591	2.71	10.60	3.36
	qSPAD-7-1	Combined data	7	10	VR7:55078511-VR7:49782591	3.45	12.06	3.39
Trichome	*qTric-3-1*	2020	3	39	VR3:7746621-VR3:2135176	2.99	6.38	0.181
	qTric-9-1	2020	9	48	VR9:5838711-VR9:11676113	2.67	6.74	0.207
	qTric-7-2	2021	7	47	VR7:50842581-VR7:14012124	6.29	14.00	−0.317
	qTric-7-2	Combined data	7	47	VR7:50842581-VR7:14012124	4.98	11.29	−0.276

Notes.

LG[a], Linkage group; Position[b], Genetic position (cM) of QTL on linkage map; Interval[c], QTL LOD support interval; LOD[d], log of odds ratio at the peak likelihood of the QTL; PVE[e], Percentage of phenotypic variation explained by individual QTL; A[f], Additive effect.

On chromosome 7, a QTL for SPAD value (*qSPAD-7-1*; VR7:55078511 and VR7:49782591; 10.60% PVE) was identified (in 2020 and 2021), while a novel QTL for trichome density (*qTric-7-2*; VR50842581 to VR14012124; 14.0% PVE) was discovered in 2021 (Fig. 2).

The combined analysis revealed detection of two QTLs, namely *qSPAD-7-* 1 for SPAD value, and *qTric-7-2* for trichome density on chromosome 7 (Fig. 3). The *qSPAD-7-1* consistently appeared independently in both years (2020 and 2021) and also in the combined data with positive additive effects from PMR-1 for SPAD value. Whereas, *qTric-7-2* was detected in 2021 and in the combined data, with negative additive effects contributed by the parent Pusa Baisakhi.

Gene ontology and candidate genes prediction of major QTLs

Two major QTLs (*qSPAD-7-1* and *qTric-7-2*) were chosen based on mapping results for gene ontology (GO) and candidate gene prediction analyses (Table S1). The genomic intervals of these QTLs were investigated, and 138 annotated genes were predicted within the 5.29 Mb physical interval of *qSPAD-7-1*, while 245 annotated genes were predicted within the 36.83 Mb interval of *qTric-7-2*. A set of 186 genes, of 383 genes located within the physical regions of two stable QTLs were selected based on the results of ShinyGO 0.77 analysis, gene annotation, and published literature and were used for further analysis (Table S2).

The study compared and validated 186 associated protein-coding genes using a BLASTN search against the *Arabidopsis* genome database. Of these, 35 genes exhibited high similarity (≥75%) to *Arabidopsis* genes and were extensively characterized (Table 3; Table S1). These genes regulate various diverse biological processes, including anatomical morphogenesis, porphyrin and chlorophyll metabolism pathways, and defense against viruses. Notably, most of the genes were from different families or coded by two genes, like Cytochrome b561 (*VRADI07G26610* and *VRADI07G09390*) and Protein trichome birefringence (*VRADI07G14170* and *VRADI07G23450*). Additionally, two genes (*VRADI07G30210* and *VRADI07G17680*) encode squamosa promoter-binding-like protein 13A, and two others (*VRADI07G10060* and *VRADI07G14740*) encode zinc finger proteins DOF5.8

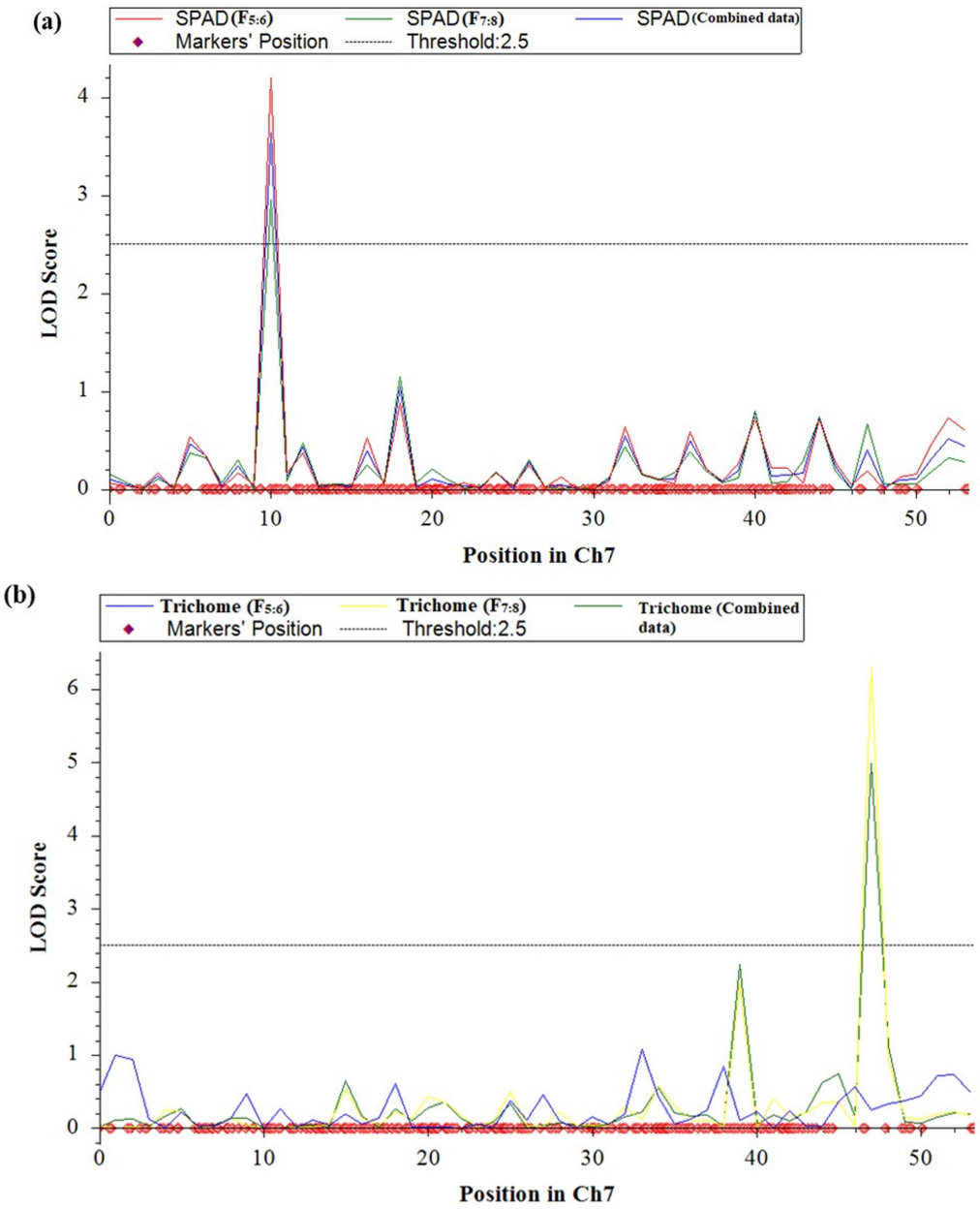

Figure 3 **LOD graphs of the identified QTLs for (A) SPAD value. (B) Trichome density derived from mungbean RILs (2020 and 2021) on the linkage maps.**

Full-size DOI: 10.7717/peerj.16722/fig-3

and DOF5.6, respectively, belonging to the zinc finger DNA-binding domain family (Table 3).

Based on GO enrichment analysis, gene annotation, and published research on chlorophyll content, three genes were identified having a role in chlorophyll biogenesis (Table 3). These genes include *VRADI07G28520* which encodes CRS2 or Chloroplast

Table 3 Details of candidate genes within two stable QTL regions for SPAD value and trichomes.

Name of QTL	Ensembl Gene ID	Position (Mbp)	Functional Annotation[a]
	VRADI07G26610	49.97	Cytochrome b561 and DOMON domain-containing protein
	VRADI07G27270	50.58	Glucose-1-phosphate adenylyltransferase large subunit 1, chloroplastic
	VRADI07G27460	50.83	outer envelope pore protein 37, chloroplastic
	VRADI07G27620	51.10	peptidyl-tRNA hydrolase, chloroplastic-like
	VRADI07G28180	51.65	Probable glutathione peroxidase 2
	VRADI07G28430	52.14	NADPH:adrenodoxin oxidoreductase, mitochondrial
	VRADI07G28520	52.29	CRS2-associated factor 1, chloroplastic-like
	VRADI07G28530	52.29	Probable glycosyltransferase isoform X1
	VRADI07G28660	52.40	senescence/dehydration-associated protein , chloroplastic (LOC106767497)
qSPAD-7-1	VRADI07G29130	52.86	ABC transporter I family member 6, chloroplastic
	VRADI07G29450	53.17	Probable inactive ATP-dependent zinc metalloprotease FTSHI 1, chloroplastic
	VRADI07G29740	53.44	6-phosphogluconate dehydrogenase, decarboxylating
	VRADI07G29860	53.57	magnesium protoporphyrin IX methyltransferase, chloroplastic
	VRADI07G30110	53.92	auxin-responsive protein SAUR71-like
	VRADI07G30210	54.07	squamosa promoter-binding-like protein 13A
	VRADI07G31080	54.98	Pentatricopeptide repeat-containing protein
	VRADI07G09390	24.96	cytochrome b561 domain-containing protein
	VRADI07G10060	26.88	Dof zinc finger protein DOF5.8
	VRADI07G14170	33.81	Protein trichome birefringence-like 12
	VRADI07G14730	34.77	DELLA protein RGL1-like (GRAS family)
	VRADI07G14740	34.79	dof zinc finger protein DOF5.6
	VRADI07G15650	36.20	transcription factor MYB86-like
	VRADI07G16030	36.88	NAC transcription factor 25-like
	VRADI07G16860	38.30	F-box/kelch-repeat protein
	VRADI07G17610	38.98	transcription factor TCP5
	VRADI07G17620	38.98	protein LONGIFOLIA 2-like isoform X1
	VRADI07G17680	39.05	Squamosa promoter-binding protein-like (SBP domain) TF family protein
	VRADI07G17740	39.12	MPB2C
	VRADI07G17780	39.17	basic helix-loop-helix (bHLH) DNA-binding superfamily protein
	VRADI07G19810	42.03	zinc finger CCCH domain-containing protein 25
	VRADI07G20260	42.56	EPIDERMAL PATTERNING FACTOR-like protein 8 isoform X1
	VRADI07G22030	44.89	transcription factor RAX1 isoform X1
	VRADI07G23450	46.56	protein trichome birefringence-like 14

(*continued on next page*)

Table 3 (*continued*)

Name of QTL	Ensembl Gene ID	Position (Mbp)	Functional Annotation[a]
	VRADI07G24840	48.19	zinc finger protein 6-like
	VRADI07G24880	48.23	COBRA-like protein 7

Notes.

[a]Candidate genes are identified using ShinyGO 0.77, Ensembl Plants, the legume information system (LIS), and available literature.

ribosomal protein S2-associated factor 1, chloroplastic-like protein belonging to YhbY-like superfamily imparting stability of chloroplast ndhA transcripts (*Li et al., 2021*); *VRADI07G29450* which encodes FTSHI1 or Filamentation Temperature-Sensitive H1 which links chloroplast biogenesis and division and belong to FtsH endopeptidase family clan MA(E) (*Kadirjan-Kalbach et al., 2012*); and *VRADI07G29860*, which encodes magnesium protoporphyrin IX methyltransferase and is involved in chlorophyll biosynthesis process and belong to S-adenosyl-L-methionine dependent methyl transferase superfamily.

For trichome development, a few transcription factors like basic Helix-Loop-Helix (bHLH), MYB102 (Myeloblastosis transcription factor 102), and Zinc finger proteins were identified. Of these, *VRADI07G24840* encodes Zinc Finger Protein 6 (ZFP6) which regulates trichome initiation through gibberellin and cytokinin signaling. The homologous gene models in *Arabidopsis*, including *AT4G25080, AT4G23940, AT5G08130*, and *AT4G21440* genes, were identified as orthologs of *VRADI07G29860, VRADI07G29450, VRADI07G17780*, and *VRADI07G15650*, respectively (Table S1).

The digital gene expression analysis revealed that the genes *AT4G25080, AT4G23940, AT5G08130, AT4G21440, AT5G47530, AT4G32360, AT2G43950, AT3G10670, AT4G18260, AT5G66940, AT1G18620* and *AT5G64470* which are the orthologs of *VRADIO7G29860, VRADIO7G29450, VRADIO7G17780, VRADIO7G15650, VRADI07G26610, VRADI07G28430, VRADI07G27460, VRADI07G29130, VRADI07G09390, VRADI07G10060, VRADI07G17620,* and *VRADI07G14170,* respectively; displayed highest expression in various plant tissues, including leaf, flower, shoot apex, young root, guard cell, trichomes, mesophyll cells, pollen tube, epidermis, etc. (Fig. 4). In addition, these genes also exhibited substantial expression in various organelles, including nucleus, mitochondria, endoplasmic reticulum, plastids, Golgi apparatus, and peroxisomes.

DISCUSSION

QTL mapping is used to map the genomic regions regulating the studied traits using correlations between markers and the phenotypic traits in a mapping population (*Takuno, Terauchi & Innan, 2012*). A few studies have identified the loci governing chlorophyll content and trichome development in plants like Arabidopsis, tomato, and soybean (*Du, Yu & Fu, 2009*; *Fang et al., 2017*; *Wang et al., 2020*). However, studies on mungbean have remained scarce. This study is an attempt to find the QTLs associated with SPAD value (chlorophyll content) and trichome density traits in mungbean. An advanced RIL population (F_6 and F_8 generations) was used having 166 lines were used for the mapping

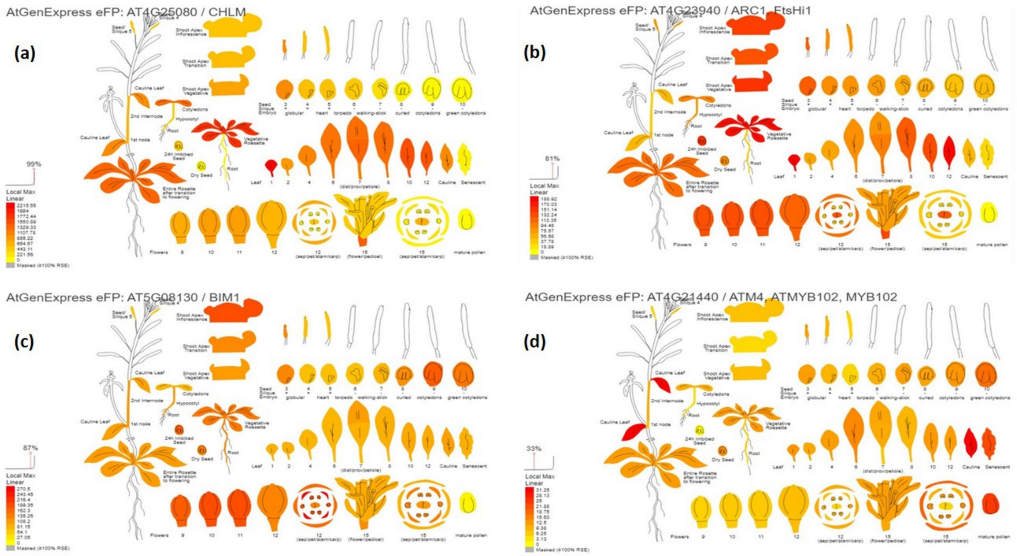

Figure 4 Digital gene expression patterns of identified candidate genes (depicted in Arabidopsis). (A) CHLM (AT4G25080) encodes magnesium protoporphyrin IX methyltransferase (orthologous to VRADIO7G29860); (B) FtsHi1 (AT4G23940) is involved in chloroplast biogenesis and division (orthologous to VRADIO7G29450); (C) BIM1 (AT5G08130) encodes bHLH transcription factors and is involved in trichome development (orthologous to VRADIO7G29450); (D) ATM4 (AT4G21440) encodes MYB86 transcription factors regulating trichome branching and elongation (corresponds to VRADIO7G15650). Expression strength is color-coded: yellow for low, while red for high.

Full-size DOI: 10.7717/peerj.16722/fig-4

using GBS. These helped in the acquisition of precise and more reliable mapping of QTLs associated with the target traits.

Variations in SPAD values and trichome traits

The RILs (Pusa Baisakhi × PMR-1) and their parents displaying significant differences in SPAD value and trichome density traits were used for precise mapping of the QTLs regulating these traits. No association was recorded between SPAD value and trichome density ($r^2 = 0.119$). Interestingly, the parents exhibited differential disease reactions (with Pusa Baisakhi being susceptible and PMR-1 resistant to MYMIV - *Mungbean Yellow Mosaic India Virus*). Trichomes do play a role in natural defense mechanisms against insects and in blackgram, a higher trichome density correlates with reduced whitefly presence (*Taggar & Gill, 2012*). Thus, there is a possibility that a RIL with high trichome density may confer enhanced whitefly tolerance and thereby MYMIV resistance to the mungbean. These findings highlight the necessity for further research to delve into the intricacies of chlorophyll content and trichome behavior in mungbean. SPAD is an indirect measure of chlorophyll content and higher chlorophyll may help, in the realization of more yield and also resistance to the MYMIV and vice versa. Previous studies have demonstrated the detrimental impact of MYMIV infection on SPAD values in mungbean (*Mishra et al., 2020*; *Dasgupta et al., 2021*).

QTLs for chlorophyll and trichome traits and their implications

Chlorophyll and trichome traits are complicated quantitative traits that are also influenced by various environmental and hereditary factors (*Du, Yu & Fu, 2009*; *Wang et al., 2020*). A single significant QTL (*qSPAD-7-1*) for SPAD value in both generations ($F_{5:6}$ and $F_{7:8}$) and also in the combined data analysis suggests that this may be governed by a few major genes and also *via* quantitative inheritance (*Du, Yu & Fu, 2009*). It could be possible that the parental lines may carry the alleles contributing to the quantitative inheritance for chlorophyll content, but these may not be sufficiently diverse in the RILs to be detected as separate QTLs. In addition, the presence of epistatic interactions among multiple genes regulating SPAD value could have masked the individual effects of other QTLs, resulting in the detection of only one significant QTL (*Messmer et al., 2009*).

Four QTLs governing SPAD value and trichome traits have been identified. For trichome, *qTric-7-2* was mapped (RIL- $F_{7:8}$) and combined data showed a PVE range of 11.29% to 14.0%. Also, two more QTLs (*qTric-3-1* and *qTric-9-1*) have been detected ($F_{5:6}$) for trichomes. For SPAD value, only one significant, major, and stable QTL (*qSPAD-7-1*; PVE: 10.60% to 12.06%) was identified ($F_{5:6}$; $F_{7:8,}$ combined data). Several studies reported mapping of SPAD or chlorophyll-related QTLs in soybean on chromosome 7 (*Yu et al., 2020*; *Wang et al., 2020*). In *Barbarea vulgaris*, *Liu et al. (2019)* identified two QTLs (*qTric-4-1* and *qTri-8-1*) for trichomes on chromosomes 4 and 8, respectively; whereas, *Byrne et al. (2017)* reported it on chromosome 7. Leaf SPAD observations are collinearly correlated with leaf chlorophyll content for several crops (*Yadava, 1986*). It is important to note that in many studies, leaf chlorophyll values measured by SPAD chlorophyll meter were found to be positively associated with grain yield (*Maiti et al., 2004*; *Kandel, 2020*). All the identified QTLs of this study are novel and mapping of SPAD value and trichome density in mungbean will aid in identifying genetic markers, understanding resistance mechanisms, facilitating marker-assisted selection, and ultimately enhancing yield.

Candidate gene analysis for SPAD value and trichomes

Identification of candidate genes is crucial for improving the target trait through the breeding approach. This study identified the candidate genes in the QTL region governing SPAD value (*qSPAD-7-1*) and trichomes (*qTric-7-2*) in mungbean. Out of the 186 genes extracted from the physical genomic interval of the two major QTLs, 35 were considered candidate genes. Network analysis has shown that the candidate genes for SPAD value are found associated with the biosynthesis of secondary metabolites, the pentose phosphate pathway, and porphyrin and chlorophyll metabolism (Fig. S2A). These genes contribute to chlorophyll formation by providing essential building blocks, coenzymes, antioxidants, and reducing power necessary for the synthesis and proper functioning of chlorophyll (*Pinto & Zempleni, 2016*; *Richter, Wang & Grimm, 2016*). Additionally, they may contribute to the plant's ability to defend against viral infections. A key candidate gene linked to *qSPAD-7-1* is *VRADI07G29860*, which is homologous to the *Arabidopsis AT4G25080* gene. This gene encodes a protein belonging to the S-adenosyl-L-methionine-dependent methyltransferase superfamily (*Richter, Wang & Grimm, 2016*). Magnesium-protoporphyrin IX methyltransferase converts magnesium-protoporphyrin IX

to magnesium-protoporphyrin IX metylester using S-adenosyl-L-methionine as a cofactor, which represents the second step in the biosynthesis of chlorophyll and bacteriochlorophyll from protoporphyrin IX.

Another important candidate gene is *VRADI07G29450*, which is homologous to the *Arabidopsis AT4G23940* gene. This encodes ATP-dependent zinc metalloprotease FTSHI1 protein, which serves as a target for several proteins involved in chlorophyll synthesis, including chlorophyllase and chlorophyll-a oxygenase (*Kadirjan-Kalbach et al., 2012*). By selectively degrading these proteins, FTSHI1 helps to maintain the balance between chlorophyll synthesis and degradation, ensuring the proper accumulation of chlorophyll in chloroplast. CRS2-associated factor 1, encoded by the *VRADI07G28520* gene (homolog of *Arabidopsis AT2G20020* gene) is a CAF1 RNA-binding CRS1/YhbY (CRM) domain-containing protein that is involved in the assembly and stabilization of chloroplast ribosomes. The chloroplast ribosome synthesizes proteins within the chloroplast, including those involved in chlorophyll biosynthesis (*Li et al., 2021*). Additionally, genes like *VRADI07G27270*, *VRADI07G27460*, *VRADI07G27620*, *VRADI07G28180*, and *VRADI07G28430*, share homology with *Arabidopsis* genes *AT5G19220*, *AT2G43950*, *AT1G18440*, *AT2G43350*, and *AT4G32360* which are involved in processes like glucose-1-phosphate adenylyltransferase activity, monoatomic ion channel activity, hydrolase activity, peroxidase activity, and oxidoreductase activity (*Goetze et al., 2006*; *Zybailov et al., 2008*; *Mugford et al., 2014*; *Attacha et al., 2017*; *Bellido et al., 2022*). These activities indirectly contribute to the overall cellular environment and metabolic processes necessary for chlorophyll synthesis (*Flores-Pérez & Jarvis, 2013*; *Cecchin et al., 2023*).

The candidate genes associated with trichomes are found associated with various processes like regulation of monopolar cell growth, cell morphogenesis, plant epidermis development, and defense response to viruses (Fig. S2B). The development and formation of trichomes are regulated by a complex network of genes and transcription factors. The *VRADI07G24840* gene (*AT1G10480* is *Arabidopsis* homolog) encodes a transcription factor ZFP5/ZFP6 which acts as the regulator of trichome initiation (*Zhou et al., 2013*). Molecular and genetic analyses suggest that ZFP6 functions upstream of ZFP8, ZFP5, and key trichome initiation regulators GL1 (GLABRA1) and GL3 (GLABRA3). ZFP6 and ZFP5 mediate the regulation of trichome initiation by integrating GA and cytokinin signaling in Arabidopsis.

Genes like *VRADI07G17780* and *VRADI07G15650*, which are homologous to the genes *AT5G08130* and *AT4G21440* in *Arabidopsis*, encode transcription factors such as basic helix-loop-helix (bHLH) family protein BIM1 (BES1-INTERACTING MYC-LIKE 1), involved in brassinosteroid signaling (*Liang et al., 2018*) and MYB102, involved in wounding and osmotic stress response (*Denekamp & Smeekens, 2003*). However, in *Arabidopsis*, other studies have shown that bHLH TFs, including GL3, ENHANCER OF GLABRA3 (EGL3), and TRANSPARENT TESTA GLABRA1 (TTG1), play a crucial role in trichome formation (*Bernhardt et al., 2003*). These factors form a protein complex known as the TTG1-GL3/EGL3-GL1 (TTG) complex, which regulates the transcriptional control of trichome development. The TTG complex functions as a positive regulator of trichome

formation by activating the expression of downstream genes involved in trichome initiation and growth.

MYB102, a MYB TF, has also been reported in *Arabidopsis*, interact with bHLH proteins to promote trichome development (*Hao et al., 2021*). MYB102 is specifically expressed in developing trichomes and acts downstream of the bHLH complex. It functions as a positive regulator of trichome branching and elongation. Other genes like *VRADI07G20260*, *VRADI07G24880*, *VRADI07G23450*, *VRADI07G14730*, and *VRADI07G17620*, which are homologous to *Arabidopsis* gene models *AT1G61120*, *AT3G16860*, *AT5G20680*, *AT2G01570*, and *AT1G18620*, contribute to the complex regulatory network underlying trichome development. They influence various aspects such as patterning, elongation, differentiation, and cell wall organization (*Attaran, Rostás & Zeier, 2008*; *Parsons et al., 2012*; *Wang et al., 2014*; *Lee et al., 2018*).

Furthermore, these candidate genes were validated using digital gene expression analysis. For SPAD value, *AT4G25080*, *AT4G23940*, and *AT2G20020*, displayed the highest expression in leaves, flowers, mesophyll, shoot apex, and various parts of the inflorescence (Figs. 4A and 4B). For trichome density, *AT1G10480*, *AT5G08130*, and *AT4G21440*, showed the highest expression in leaves, flowers, young roots, guard cells, trichomes, pollen tubes, and epidermis (Figs. 4C and 4D). *Reddy et al. (2020)* also validated a few key genes in mungbean through digital gene expression analysis for phosphorus use efficiency traits. In the future, by targeted manipulation of identified candidate genes *via* genetic engineering or gene editing tools, desired changes in chlorophyll content and trichome density can be induced for the incorporation of MYMIV resistance and enhanced yield.

CONCLUSIONS

This study comprehends the genetic foundations of traits like SPAD value (chlorophyll content) and trichome density, in mungbean. The QTL mapping has identified the genomic regions governing SPAD value and trichome density traits. The study identified 35 candidate genes in two major QTLs viz., *qSPAD-7-1* and *qTric-7-2* which govern SPAD value and trichome density in mungbean, respectively. The identified QTLs can be used for trait enhancement through dedicated breeding efforts. The mapped QTL for trichome density spanned a distance of nearly 36 Mb which prompts consideration for future investigations, where efforts may be directed towards refining the resolution of this mapping to pinpoint the specific gene governing this trait.

ACKNOWLEDGEMENTS

The technical support received by Mr. Dilip Kumar (Indian Agricultural Research Institute, New Delhi) is duly acknowledged.

ADDITIONAL INFORMATION AND DECLARATIONS

Funding

This research was funded by the Indian Council of Agricultural Research (ICAR), New Delhi, and SERB (Science and Engineering Research Board), New Delhi (CRG/2019/002024). Ramakrishnan M. Nair received funding from the long-term strategic donors of the World Vegetable Center: Taiwan, the United States Agency for International Development (USAID), the UK Government's Foreign, Commonwealth & Development Office (FCDO), the Australian Centre for International Agricultural Research (ACIAR), Germany, Thailand, Philippines, Korea, Japan, and funding from the ACIAR Project on International Mungbean Improvement Network (CROP/2019/144). The funders had no role in study design, data collection and analysis, decision to publish, or preparation of the manuscript.

Grant Disclosures

The following grant information was disclosed by the authors:
Indian Council of Agricultural Research (ICAR), New Delhi.
SERB (Science and Engineering Research Board), New Delhi: CRG/2019/002024.
World Vegetable Center: Taiwan.
The United States Agency for International Development (USAID).
The UK Government's Foreign, Commonwealth & Development Office (FCDO).
Australian Centre for International Agricultural Research (ACIAR).
ACIAR Project on International Mungbean Improvement Network: CROP/2019/144.

Competing Interests

The authors declare there are no competing interests.

Author Contributions

- Nikki Kumari performed the experiments, analyzed the data, prepared figures and/or tables, authored or reviewed drafts of the article, and approved the final draft.
- Gyan Prakash Mishra conceived and designed the experiments, authored or reviewed drafts of the article, and approved the final draft.
- Harsh Kumar Dikshit conceived and designed the experiments, authored or reviewed drafts of the article, and approved the final draft.
- Soma Gupta performed the experiments, prepared figures and/or tables, and approved the final draft.
- Anirban Roy performed the experiments, analyzed the data, prepared figures and/or tables, and approved the final draft.
- Subodh Kumar Sinha analyzed the data, prepared figures and/or tables, and approved the final draft.
- Dwijesh C. Mishra analyzed the data, prepared figures and/or tables, and approved the final draft.
- Shouvik Das performed the experiments, analyzed the data, prepared figures and/or tables, and approved the final draft.

- Ranjeet R. Kumar analyzed the data, prepared figures and/or tables, and approved the final draft.
- Ramakrishnan Madhavan Nair conceived and designed the experiments, authored or reviewed drafts of the article, and approved the final draft.
- Muraleedhar Aski conceived and designed the experiments, analyzed the data, authored or reviewed drafts of the article, and approved the final draft.

DNA Deposition

The following information was supplied regarding the deposition of DNA sequences:

The sequence data are available at GenBank: PRJNA914895.

Data Availability

The following information was supplied regarding data availability:

The raw data for two-year SPAD values and Trichome data are available in the Supplemental Files.

Supplemental Information

Supplemental information for this article can be found online at http://dx.doi.org/10.7717/peerj.16722#supplemental-information.

REFERENCES

All India Coordinated Research Project (AICRP). 2022. All India Coordinated Research Project on MULLaRP (Mungbean, Urdbean, Lentil, Lathyrus, Rajmash and Pea) Project Coordinator's Report, ICAR-Indian Institute of Pulses Research, Kanpur–208024. *Available at https://iipr.icar.gov.in/wp-content/uploads/2023/07/PC-Report-MULLaRP_Rabi_2021-22.pdf* .

Angira B, Zhang Y, Zhang Y, Scheuring CF, Masor L, Coleman J, Singh BB, Zhang HB, Hays DB, Zhang M, Khanal M, Correa E, Bhatta BP, Malla S. 2022. Genetic dissection of iron deficiency chlorosis by QTL analysis in cowpea. *Euphytica* **218**:38 DOI 10.1007/s10681-022-02989-y.

Attacha S, Solbach D, Bela K, Moseler A, Wagner S, Schwarzländer M, Aller I, Müller SJ, Meyer AJ. 2017. Glutathione peroxidase-like enzymes cover five distinct cell compartments and membrane surfaces in *Arabidopsis thaliana*. *Plant, Cell and Environment* **40(8)**:1281–1295 DOI 10.1111/pce.12919.

Attaran E, Rostás M, Zeier J. 2008. Pseudomonas syringae elicits emission of the terpenoid (E, E)-4, 8 12-trimethyl-1, 3 7, 11-tridecatetraene in *Arabidopsis* leaves *via* jasmonate signaling and expression of the terpene synthase TPS4. *Molecular Plant-Microbe Interactions* **21(11)**:1482–1497 DOI 10.1094/MPMI-21-11-1482.

Atwell S, Huang YS, Vilhjalmsson BJ, Willems G, Horton M, Li Y, Meng DZ, Platt A, Tarone AM, Hu TT, Jiang R, Muliyati NW, Zhang X, Amer MA, Baxter I, Brachi B, Chory J, Dean C, Debieu MD, Meaux J, Ecker JR, Faure N, Kniskern JM, Jones JDG, Michael T, Nemri A, Roux F, Salt DE, Tang C, Todesco M, Traw MB, Weigel D, Marjoram P, Borevitz JO, Bergelson J, Nordborg M. 2010. Genome-wide

association study of 107 phenotypes in *Arabidopsis thaliana* inbred lines. *Nature* **465**:627–631 DOI 10.1038/nature08800.

Austin RS, Hiu S, Waese J, Ierullo M, Pasha A, Wang TT, Fan J, Foong C, Breit R, Desveaux D, Moses A, Provart NJ. 2016. New BAR tools for mining expression data and exploring Cis-elements in *Arabidopsis thaliana*. *Plant Journal* **88**:490–504 DOI 10.1111/tpj.13261.

Bellido AM, Distéfano AM, Setzes N, Cascallares MM, Oklestkova J, Novak O, Pagnussat GC. 2022. A mitochondrial ADXR–ADX–P450 electron transport chain is essential for maternal gametophytic control of embryogenesis in *Arabidopsis*. *Proceedings of the National Academy of Sciences of the United States of America* **119(4)**:e2000482119.

Bernhardt C, Lee MM, Gonzalez A, Zhang F, Lloyd A, Schiefelbein J. 2003. The bHLH genes GLABRA3 (GL3) and ENHANCER OF GLABRA3 (EGL3) specify epidermal cell fate in the *Arabidopsis* root. *Development* **130(26)**:6431–6439 DOI 10.1242/dev.00880.

Byrne SL, Erthmann PO, Agerbirk N, Bak S, Hauser TP, Nagy I, Paina C, Asp T. 2017. The genome sequence of *Barbarea vulgaris* facilitates the study of ecological biochemistry. *Scientific Reports* **7**:1 DOI 10.1038/s41598-016-0028-x.

Carter GA, Knapp AK. 2001. Leaf optical properties in higher plants: linking spectral characteristics to stress and chlorophyll concentration. *American Journal of Botany* **88(4)**:677–684 DOI 10.2307/2657068.

Cecchin M, Simicevic J, Chaput L, Hernandez Gil M, Girolomoni L, Cazzaniga S, Remacle C, Hoeng J, Ivanov NV, Titz B, Ballottari M. 2023. Acclimation strategies of the green alga Chlorella vulgaris to different light regimes revealed by physiologic and comparative proteomic analyses. *Journal of Experimental Botany* **74(15)**:4540–4558 DOI 10.1093/jxb/erad170.

Chen T, Hu L, Wang S, Wang L, Cheng X, Chen H. 2022. Construction of high-density genetic map and identification of a bruchid resistance locus in mung bean (*Vigna radiata* L.). *Frontiers in Genetics* **13**:903267 DOI 10.3389/fgene.2022.903267.

Chen Z, Zheng Z, Luo W, Zhou H, Ying Z, Liu C. 2021. Detection of a major QTL conditioning trichome length and density on chromosome arm 4BL and development of near isogenic lines targeting this locus in bread wheat. *Molecular Breeding* **41**:10 DOI 10.3389/fgene.2022.903267.

Dasgupta U, Mishra GP, Dikshit HK, Mishra DC, Bosamia T, Roy A, Bhati J, Priti , Aski A, Kumar RR, Singh AK, Kumar A, Sinha SK, Chaurasia S, Praveen S, Nair RM. 2021. Comparative RNA-Seq analysis unfolds a complex regulatory network imparting yellow mosaic disease resistance in mungbean [*Vigna radiata* (L.) R. Wilczek]. *PLOS ONE* **16(1)**:e0244593 DOI 10.1371/journal.pone.0244593.

Denekamp M, Smeekens SC. 2003. Integration of wounding and osmotic stress signals determines the expression of the AtMYB102 transcription factor gene. *Plant Physiology* **132(3)**:1415–1423 DOI 10.1104/pp.102.019273.

Dhanapal AP, Ray JD, Singh SK, Hoyos-Villegas V, Smith JR, Purcell LC, Fritschi FB. 2016. Genome-wide association mapping of soybean chlorophyll traits based

on canopy spectral reflectance and leaf extracts. *BioMed Central Plant Biology* **16(1)**:1–15.

Du W-j, Yu D-y, Fu S-x. 2009. Analysis of QTLs for the trichome density on the upper and downer surface of leaf blade in soybean [*Glycine max* (L.) Merr.]. *Agricultural Sciences in China* **8(5)**:529–537 DOI 10.1016/S1671-2927(08)60243-6.

Elshire RJ, Glaubitz JC, Sun Q, Poland JA, Kawamoto K, Buckler ES, Mitchell SE. 2011. A robust, simple genotyping-by-sequencing (GBS) approach for high diversity species. *PLOS ONE* **6(5)**:e19379 DOI 10.1371/journal.pone.0019379.

Fang C, Ma Y, Wu S, Liu Z, Wang Z, Yang R, Hu G, Zhou Z, Yu H, Zhang M, Pan Y, Zhou G, Ren H, Du W, Yan H, Wang Y, Han D, Shen Y, Liu S, Liu T, Zhang J, Qin H, Yuan J, Yuan X, Kong F, Liu B, Li J, Zhang J, Wang G, Zhu B, Tian Z. 2017. Genome-wide association studies dissect the genetic networks underlying agronomical traits in soybean. *Genome Biology* **18**:1 DOI 10.1186/s13059-016-1139-1.

Flores-Pérez Ú, Jarvis P. 2013. Molecular chaperone involvement in chloroplast protein import. *Biochimica et Biophysica Acta (BBA)-Molecular Cell Research* **1833(2)**:332–340 DOI 10.1016/j.bbamcr.2012.03.019.

Goetze TA, Philippar K, Ilkavets I, Soll J, Wagner R. 2006. OEP37 is a new member of the chloroplast outer membrane ion channels. *Journal of Biological Chemistry* **281(26)**:17989–17998 DOI 10.1074/jbc.M600700200.

Grant JR, Arantes AS, Liao X, Stothard P. 2011. In-depth annotation of SNPs arising from resequencing projects using NGS-SNP. *Bioinformatics* **27(16)**:2300–2301 DOI 10.1093/bioinformatics/btr372.

Guang-Jun LI, He-Nan LI, Cheng LG, Zhang YM. 2010. QTL analysis for dynamic expression of SPAD value in soybean (*Glycine max* L. Merr.). *Acta Agronomica Sinica* **36(2)**:242–248.

Hao Y, Zong X, Ren P, Qian Y, Fu A. 2021. Basic Helix-Loop-Helix (bHLH) transcription factors regulate a wide range of functions in *Arabidopsis*. *International Journal of Molecular Sciences* **22(13)**:7152 DOI 10.3390/ijms22137152.

Jiang BZ, Cheng YB, Cai ZD, Li M, Jiang Z, Ma RR, Yuan YS, Xia QJ, Nian H. 2020. Fine mapping of a Phytophthora-resistance locus RpsGZ in soybean using genotyping-by-sequencing. *BioMed Central Genomics* **21**:1–11.

Kadirjan-Kalbach DK, Yoder DW, Ruckle ME, Larkin RM, Osteryoung KW. 2012. FtsHi1/ARC1 is an essential gene in *Arabidopsis* that links chloroplast biogenesis and division. *The Plant Journal* **72(5)**:856–867 DOI 10.1111/tpj.12001.

Kandel BP. 2020. SPAD value varies with age and leaf of maize plant and its relationship with grain yield. *BioMed Central Research Notes* **13(1)**:475 DOI 10.1186/s13104-020-05324-7.

Kariyat RR, Hardison SB, Ryan AB, Stephenson AG, De Moraes CM, Mescher MC. 2018. Leaf trichomes affect caterpillar feeding in an instar-specific manner. *Communicative and Integrative Biology* **11(3)**:1–6 DOI 10.1080/19420889.2018.1486653.

Kirik V, Simon M, Huelskamp M, Schiefelbein J. 2004. The enhancer of try and CPC1 gene acts redundantly with TRIPTYCHON and CAPRICE in trichome and

root hair cell patterning in *Arabidopsis*. *Developmental Biology* **268(2)**:506–513 DOI 10.1016/j.ydbio.2003.12.037.

Kivimaki M, Karkkainen K, Gaudeul M, Loe G, Agren J. 2007. Gene, phenotype and function: GLABROUS1 and resistance to herbivory in natural populations of *Arabidopsis lyrata*. *Molecular Ecology* **16(2)**:453–462 DOI 10.1111/j.1365-294X.2007.03109.x.

Lee YK, Rhee JY, Lee SH, Chung GC, Park SJ, Segami S, Maeshima M, Choi G. 2018. Functionally redundant LNG3 and LNG4 genes regulate turgor-driven polar cell elongation through activation of XTH17 and XTH24. *Plant Molecular Biology* **97**:23–36 DOI 10.1007/s11103-018-0722-0.

Li X, Luo W, Zhou W, Yin X, Wang X, Li X, Jiang C, Zhang Q, Kang X, Zhang A, Zhang Y, Lu C. 2021. CAF proteins help SOT1 regulate the stability of chloroplast ndhA transcripts. *International Journal of Molecular Sciences* **22(23)**:12639 DOI 10.3390/ijms222312639.

Liang T, Mei S, Shi C, Yang Y, Peng Y, Ma L, Wang F, Li X, Huang X, Yin Y, Liu H. 2018. UVR8 interacts with BES1 and BIM1 to regulate transcription and photomorphogenesis in Arabidopsis. *Developmental Cell* **44(4)**:512–523 DOI 10.1016/j.devcel.2017.12.028.

Liu TJ, Zhang YJ, Agerbirk N, Wang HP, Wei XC, Song JP, He HJ, Zhao XZ, Zhang XH, Li XX. 2019. A high-density genetic map and QTL mapping of leaf traits and glucosinolates in *Barbarea vulgaris*. *BioMed Central Genomics* **20(1)**:371 DOI 10.1186/s12864-019-5769-z.

Lodhi MA, Ye GN, Weeden NF, Reisch BI. 1994. A simple and efficient method for DNA extraction from grapevine cultivars and Vitis species. *Plant Molecular Biology Reporter* **12(1)**:6–13 DOI 10.1007/BF02668658.

Lombard K, O'Neill M, Mexal J, Ulery A, Onken B, Bettmann G, Heyduck R. 2010. Can soil plant analysis development values predict chlorophyll and total Fe in hybrid poplar? *Agroforestry Systems* **78**:1–11 DOI 10.1007/s10457-009-9214-1.

Ma BL, Morrison MJ, Voldeng HD. 1995. Leaf greenness and photosynthetic rates in soybean. *Crop Science* **35(5)**:1411–1414 DOI 10.2135/cropsci1995.0011183X003500050025x.

Maiti D, Das DK, Karak T, Banerjee M. 2004. Management of nitrogen through the use of leaf color chart (LCC) and soil plant analysis development (SPAD) or chlorophyll meter in rice under irrigated ecosystem. *The Scientific World Journal* **4**:838–846 DOI 10.1100/tsw.2004.137.

Markwell J, Osterman JC, Mitchell JL. 1995. Calibration of the Minolta SPAD-502 leaf chlorophyll meter. *Photosynthesis Research* **46**:467–472 DOI 10.1007/BF00032301.

Mathivathana MK, Murukarthick J, Karthikeyan A, Jang W, Dhasarathan M, Jagadeeshselvam N, Sudha M, Vanniarajan C, Karthikeyan G, Yang TJ, Raveendran M, Pandiyan M, Senthil N. 2019. Detection of QTLs associated with mungbean yellow mosaic virus (MYMV) resistance using the interspecific cross of *Vigna radiate* × *Vigna umbellata*. *Journal of Applied Genetics* **60**:255–268 DOI 10.1007/s13353-019-00506-x.

Mauricio R. 2005. Ontogenetics of QTL: the genetic architecture of trichome density over time in *Arabidopsis thaliana*. *Genetics of Adaptation* **123(1-2)**:75–85.

Messmer R, Fracheboud Y, Bänziger M, Vargas M, Stamp P, Ribaut JM. 2009. Drought stress and tropical maize: QTL-by-environment interactions and stability of QTLs across environments for yield components and secondary traits. *Theoretical and Applied Genetics* **119**:913–930 DOI 10.1007/s00122-009-1099-x.

Mishra GP, Dikshit HK, Ramesh SV, Tripathi K, Kumar RR, Aski M, Singh A, Roy A, Priti , Kumari N, Dasgupta U, Kumar A, Praveen S, Nair RM. 2020. Yellow mosaic disease (YMD) of mungbean (*Vigna radiata* (L.) Wilczek): Current status and management opportunities. *Frontiers in Plant Science* **11**:918 DOI 10.3389/fpls.2020.00918.

Mugford ST, Fernandez O, Brinton J, Flis A, Krohn N, Encke BB, Feil R, Sulpice R, Lunn JE, Stitt M, Smith AM. 2014. Regulatory properties of ADP glucose pyrophosphorylase are required for adjustment of leaf starch synthesis in different photoperiods. *Plant Physiology* **166(4)**:1733–1747 DOI 10.1104/pp.114.247759.

Parsons HT, Christiansen K, Knierim B, Carroll A, Ito J, Batth TS, Smith-Moritz AM, Morrison S, McInerney P, Hadi MZ, Auer M, Mukhopadhyay A, Petzold CJ, Scheller HV, Loqué D, Heazlewood JL. 2012. Isolation and proteomic characterization of the Arabidopsis Golgi defines functional and novel components involved in plant cell wall biosynthesis. *Plant Physiology* **159(1)**:12–26 DOI 10.1104/pp.111.193151.

Pinto JT, Zempleni J. 2016. Riboflavin. *Advances in Nutrition* **7(5)**:973–975 DOI 10.3945/an.116.012716.

Priti , Mishra GP, Dikshit HK, Vinutha T, Mechiya T, Stobdan T, Sangwan S, Aski M, Singh A, Kumar RR, Tripathi K, Kumar S, Nair RM, Praveen S. 2021. Diversity in phytochemical composition, antioxidant capacities, and nutrient contents among mungbean and lentil microgreens when grown at plain-altitude region (Delhi) and high-altitude region (Leh-Ladakh), India. *Frontiers in Plant Sciences* **12**:710812 DOI 10.3389/fpls.2021.710812.

Priti , Sangwan S, Kukreja B, Mishra GP, Dikshit HK, Singh A, Aski M, Kumar A, Taak Y, Stobdan T, Das S, Kumar RR, Yadava DK, Praveen S, Kumar S, Nair RM. 2022. Yield optimization, microbial load analysis, and sensory evaluation of mungbean (*Vigna radiata* L.), lentil (*Lens culinaris* subsp. culinaris), and Indian mustard (*Brassica juncea* L.) microgreens grown under greenhouse conditions. *PLOS ONE* **17(5)**:e0268085 DOI 10.1371/journal.pone.0268085.

Qi XP, Li MW, Xie M, Liu X, Ni M, Shao GH, Song C, Kay-Yuen YA, Tao Y, Wong FL, Isobe S, Wong CF, Wong KS, Xu C, Li C, Wang Y, Guan R, Sun F, Fan G, Xiao Z, Zhou F, Phang TH, Liu X, Tong SW, Chan TF, Yiu SM, Tabata S, Wang J, Xu X, Lam HM. 2014. Identification of a novel salt tolerance gene in wild soybean by whole-genome sequencing. *Nature Communication* **5**:4340 DOI 10.1038/ncomms5340.

R Core Team. 2013. R: A language and environment for statistical computing. Vienna: R Foundation for Statistical Computing. *Available at http://www.R-project.org/*.

Reddy VRP, Das S, Dikshit HK, Mishra GP, Aski M, Meena SK, Singh A, Pandey R, Singh MP, Tripathi K, Gore PG, Priti , Bhagat TK, Kumar S, Nair R, Sharma TR. 2020. Genome wide association analysis for phosphorus use efficiency traits in mungbean (*Vigna radiata* L. Wilczek) using genotyping by sequencing approach. *Frontiers in Plant Sciences* **11**:537766 DOI 10.3389/fpls.2020.537766.

Reddy VRP, Das S, Dikshit HK, Mishra GP, Aski M, Singh A, Tripathi K, Pandey R, Bansal R, Singh MP, Gore PG, Manjunatha PB, Kothari D, Rai N, Nair RM. 2021. Genetic dissection of phosphorous uptake and utilization efficiency traits using GWAS in mungbean. *Agronomy* **11(7)**:1401 DOI 10.3390/agronomy11071401.

Richter AS, Wang P, Grimm B. 2016. Arabidopsis Mg-protoporphyrin IX methyltransferase activity and redox regulation depend on conserved cysteines. *Plant and Cell Physiology* **57(3)**:519–527 DOI 10.1093/pcp/pcw007.

Roberts JJ, Gallun RL, Patterson FL, Foster JE. 1979. Effects of wheat leaf pubescence on the Hessian fly. *Journal of Economic Entomology* **72(2)**:211–214 DOI 10.1093/jee/72.2.211.

Sakowska K, Alberti G, Genesio L, Peressotti A, Delle Vedove G, Gianelle D, Colombo R, Rodeghiero M, Panigada C, Juszczak R, Celesti M, Rossini M, Haworth M, Campbell BW, Mevy JP, Vescovo L, Cendrero-Mateo MP, Rascher U, Miglietta F. 2018. Leaf and canopy photosynthesis of a chlorophyll deficient soybean mutant. *Plant, Cell and Environment* **41(6)**:1427–1437 DOI 10.1111/pce.13180.

Schillinger Jr JA, Gallun RL. 1968. Leaf pubescence of wheat as a deterrent to the cereal leaf beetle, Oulema melanopus. *Annals of the Entomological Society of America* **61(4)**:900–903 DOI 10.1093/aesa/61.4.900.

Singhal GS, Renger G, Sopory SK, Irrgang KD (eds.) 2012. *Concepts in photobiology: photosynthesis and photomorphogenesis*. XV. Dordrecht: Springer, 1019 DOI 10.1007/978-94-011-4832-0.

Stam P. 1993. Construction of integrated genetic linkage maps by means of a new computer package: Join Map. *The Plant Journal* **3(5)**:739–744 DOI 10.1111/j.1365-313X.1993.00739.x.

Taggar GK, Gill RS. 2012. Preference of whitefly, Bemisia tabaci, towards black gram genotypes: role of morphological leaf characteristics. *Phytoparasitica* **40**:461–474 DOI 10.1007/s12600-012-0247-z.

Takuno S, Terauchi R, Innan H. 2012. The power of QTL mapping with RILs.

Voorrips RE. 2022. MapChart: software for the graphical presentation of linkage maps and QTLs. *Journal of Heredity* **93(1)**:77–78 DOI 10.1093/jhered/93.1.77.

Wang L, Conteh B, Fang L, Xia Q, Nian H. 2020. QTL mapping for soybean (*Glycine max* L.) leaf chlorophyll-content traits in a genotyped RIL population by using RAD-seq based high-density linkage map. *BioMed Central Genomics* **21**:1–18.

Wang W, Zhang J, Qin Q, Yue J, Huang B, Xu X, Yan L, Hou S. 2014. The six conserved serine/threonine sites of REPRESSOR OF ga1-3 protein are important for its functionality and stability in gibberellin signaling in *Arabidopsis*. *Planta* **240**:763–779 DOI 10.1007/s00425-014-2113-3.

Yadava UL. 1986. A rapid and nondestructive method to determine chlorophyll in intact leaves. *HortScience* **21(6)**:1449–1450 DOI 10.21273/HORTSCI.21.6.1449.

Yasmin S, Ali M, Rahman MM, Akter MS, Paul AK, Akter MM, Latif MA. 2022. Screening certain mungbean varieties against thrips (Thysanoptera: Thripidae) and exploration of resistance sources. *Agrosystems, Geosciences and Environment* **5(3)**:e20287 DOI 10.1002/agg2.20287.

Yu K, Wang J, Sun C, Liu X, Xu H, Yang Y, Dong L, Zhang D. 2020. High-density QTL mapping of leaf-related traits and SPAD value in three soybean RIL populations. *BioMed Central Plant Biology* **20(1)**:470 DOI 10.1186/s12870-020-02684-x.

Yu M, Huang L, Feng N, Zheng D, Zhao J. 2022. Exogenous uniconazole enhances tolerance to chilling stress in mung beans (*Vigna radiata* L.) through cross talk among photosynthesis, antioxidant system, sucrose metabolism, and hormones. *Journal of Plant Physiology* **276**:153772 DOI 10.1016/j.jplph.2022.153772.

Zeng ZB. 1993. Theoretical basis for separation of multiple linked gene effects in mapping quantitative trait loci. *Proceedings of the National Academy of Sciences of the United States of America* **90(23)**:10972–10976.

Zhao M, Morohashi K, Hatlestad G, Grotewold E, Lloyd A. 2008. The TTG1-bHLH-MYB complex controls trichome cell fate and patterning through direct targeting of regulatory loci. *Development* **135(11)**:1991–1999 DOI 10.1242/dev.016873.

Zhou Z, Sun L, Zhao Y, An L, Yan A, Meng X, Gan Y. 2013. Zinc Finger P rotein 6 (ZFP 6) regulates trichome initiation by integrating gibberellin and cytokinin signaling in *Arabidopsis thaliana*. *New Phytologist* **198(3)**:699–708 DOI 10.1111/nph.12211.

Zybailov B, Rutschow H, Friso G, Rudella A, Emanuelsson O, Sun Q, Van Wijk KJ. 2008. Sorting signals, N-terminal modifications and abundance of the chloroplast proteome. *PLOS ONE* **3(4)**:e1994 DOI 10.1371/journal.pone.0001994.